Weak Influence of Divalent Ions on Anionic Surfactant Surface-Aggregation

ARTICLE *in* LANGMUIR · MARCH 1997

Impact Factor: 4.46 · DOI: 10.1021/la960861e

2 AUTHORS:

Erica J Wanless
University of Newcastle
81 PUBLICATIONS **2,511** CITATIONS
SEE PROFILE

William Ducker
Virginia Tech
124 PUBLICATIONS **6,589** CITATIONS
SEE PROFILE

Weak Influence of Divalent Ions on Anionic Surfactant Surface-Aggregation

Erica J. Wanless and William A. Ducker*

Department of Chemistry, University of Otago, P.O. Box 56, Dunedin, New Zealand

Received September 4, 1996. In Final Form: December 12, 1996[⊗]

The aggregated structure of sodium dodecyl sulfate (SDS) adsorbed to the graphite−solution interface has been determined in the presence of the divalent ions: Mg^{2+}, Mn^{2+}, and Ca^{2+}. Divalent ions are expected to alter the electrostatic interactions between charged headgroups and thus to cause changes from the structure formed with monovalent ions. However, atomic force microscopy reveals that the adsorbed structures are long (μm) and thin (~5 nm) and thus very similar in appearance to those observed in the presence of only monovalent counterions. Energetic considerations suggest that under most conditions the aggregates are hemicylinders, although not necessarily of constant curvature. When Mn^{2+} is added at constant low SDS concentration, the narrow dimension of the structure (the period) decreases linearly with solution Debye length down to a limiting period of about 5 nm. When Mg^{2+} is added at constant low SDS concentration, the period decreases slightly and then remains roughly constant. This suggests that the aggregate diameter increases. For both of these ions, force measurements suggests that there is a transition from a thin layer to a thicker layer as the divalent ion is added. At surfactant concentrations several times greater than the critical micelle concentration, the addition of divalent ions has no observable effect on the adsorption. We did not observe a transition to a flat layer at any of the conditions examined.

Introduction

Electrostatic forces play a crucial role in determining phase equilibria in systems containing ionic surfactants. The shape of an ionic surfactant aggregate in solution is dominated by the minimization of two interactions: the hydrocarbon−water interaction, and the repulsive electrostatic interaction between similarly charged headgroups. The balance between these forces can be perturbed by a change in the intermolecular forces as a result of different solution conditions such as an increase in surfactant concentration, addition of an electrolyte, or a change in temperature. Additional electrolyte screens the electrostatic repulsion between headgroups, thus permitting the headgroups to move closer together. This results in an aggregate of different mean curvature and sometimes a phase transition from one self-assembled structure to another.[1,2] For example, sodium dodecyl sulfate (SDS) forms spherical micelles above the critical micelle concentration (cmc) of 8.1 mM and also undergoes a transition to cylindrical micelles in 0.8 M NaCl at 0.45 M SDS.[3]

Divalent counterions are expected to be more effective than monovalent ions in screening electrostatic interactions and reducing surfactant headgroup area because (a) a greater charge screens more effectively, (b) each divalent ion is more strongly attracted to an aggregate, and (c) divalent ions can sometimes cause charge reversal. Wennerström *et al.*[4] have reviewed the electrostatic effects of divalent ions on aggregation in bulk. In some cases, there are significant differences in phase behavior between systems with monovalent and divalent counterions. For example, reverse hexagonal phases occur in both magnesium and calcium dodecyl sulfate/decanol/water systems, but not in the SDS/decanol/water system.[5] Also, the swelling capability of lamellar phases of bis(2-ethylhexyl) sulfosuccinate is reduced in the presence of Ca^{2+} considerably more than expected on the basis of the Poisson−Boltzmann ion distribution.[6] The strong effect of divalent ions was attributed to ion-correlation induced deviations leading to a net electrostatic attraction.[6] Divalent counterions, however, frequently have surprisingly little effect on surfactant aggregates: Ca^{2+} and Mg^{2+} do not result in growth of octyl sulfate micelles (spherical) nor do they promote a transition to cylindrical micelles.[7] Similarly, SO_4^{2-} does not promote a transition of spherical hexadecyltrimethylammonium micelles to cylindrical micelles.[8] The weak influence of divalent ions in these instances was attributed to deviations from the expected ion distribution due to a greater repulsion of the divalent ions away from the low dielectric region of the micelle interior.[4]

The forces which lead to self-assembly in bulk are also present at the solid−solution interface, so it is reasonable to expect that surfactants will aggregate at the interface. This has recently been directly confirmed by Manne *et al.*[9] using atomic force microscopy (AFM) on solid substrates. AFM can resolve forces on a length scale smaller than the radius of a micelle (~5 nm) and thus can be used to directly image the shape of surface aggregates. The general features of surface aggregation have been studied for quaternary ammonium surfactants[10] and a zwitterionic surfactant[11] on both hydrophobic and hydrophilic substrates and for mixtures of cationic and zwitterionic surfactants on mica.[12] We have also studied the aggregation of SDS on graphite.[13]

* To whom correspondence should be addressed: e-mail, duck@alkali.otago.ac.nz.

[⊗] Abstract published in *Advance ACS Abstracts,* February 1, 1997.

(1) Israelachvili, J. N.; Mitchell, D. J; Ninham, B. W. *J. Chem. Soc., Faraday Trans. 1,* **1976**, *72,* 1525−1568.

(2) Israelachvili, J. N. *Intermolecular and Surface Forces*, 2nd ed.; Academic Press: London, 1992.

(3) Hayashi, S.; Ikeda, S. *J. Phys. Chem.* **1980**, *84,* 744−751.

(4) Wennerström, H.; Khan, A.; Lindman, B. *Adv. Colloid Interface Sci.* **1991**, *34,* 433−449.

(5) Maciejewska, D.; Khan, A.; Lindman, B. *Colloid Polym. Sci.* **1986**, *264,* 909−916.

(6) Khan, A.; Jönsson, B.; Wennerström, H. *J. Phys. Chem.* **1985**, 89, 5180−5184.

(7) Lindström, B.; Khan, A.; Söderman, O.; Kamenka, N.; Lindman, B. *J. Phys. Chem.* **1985**, *89*, 5313−5318.

(8) Maciejewska, D.; Khan, A.; Lindman, B. *Prog. Colloid Polym. Sci.* **1987**, *73*, 174−179.

(9) Manne, S.; Cleveland, J. P.; Gaub, H. E.; Stucky, G. D.; Hansma, P. K. *Langmuir* **1994**, *10*, 4409−4413.

(10) Manne, S.; Gaub, H. E. *Science* **1995**, *270*, 1480−1482.

(11) Ducker, W. A.; Grant, L. M. *J. Phys. Chem.* **1996**, *100*, 11507−11511.

S0743-7463(96)00861-X CCC: $14.00

Although the process of aggregation at an interface is similar to that occurring in bulk, the interface can exert strong forces on the surfactant. For example, the substrate can exert influence via electrostatic forces and/or hydrogen bonding. These forces cause the surface activity for which surfactants are so important. In addition, the substrate modifies the aggregate environment by introducing a dielectric discontinuity, a new geometry, and a change in the entropy of mixing. These contributions can result in a solution surface reconstruction with surface aggregates of different shape to those found in bulk.

In this work we present an AFM investigation of the effect of divalent ions on the aggregation of dodecyl sulfate on graphite. A convenient way of varying the electrostatic contribution to the surface self-assembly is to determine the effect of adding electrolyte to a known system. In isotherm studies, the addition of Na^+ has been shown to increase the adsorption of dodecyl sulfate on graphon (a graphitic material) in SDS solutions by 25%,[14] and the addition of Ca^{2+} doubled the adsorption.[15,16] We have previously studied the shape of surface aggregates of dodecyl sulfate in pure surfactant solutions and in NaCl.[13] In pure SDS solutions more concentrated than 2.8 mM, the surfactant was found to assemble in an organized periodic structure consisting of long parallel aggregates. The lowest concentration at which aggregation was observed has been termed the surface aggregation concentration (sac). The aggregates appear as uninterrupted parallel stripes in the AFM images and are observed when the tip and the solid substrate are slightly separated. The exact separation between the tip and the surface aggregates is difficult to quantify because the space occupied by the surfactant is ill-defined and is a function of the force applied by the tip during imaging. There is always an upper limit to the force which can be applied above which the AFM image is dominated by the features of the substrate.

For SDS solutions, the shape of the adsorbed dodecyl sulfate aggregates on graphite was not significantly altered when the surfactant concentration was increased above the sac, but rather the period of the adsorbate structure decreased.[13] This decrease in period mirrored the increase in adsorption density shown in the isotherm.[14] When NaCl was added at constant SDS concentration, there was still no change in aggregate morphology, but the period of the adsorbate decreased approximately linearly with the Debye length of the solution. This implies that electrostatic repulsion between the adsorbed aggregates is one of the dominant forces dictating the aggregate period.

In this work, we extend our study of the morphology of dodecyl sulfate at the graphite−solution interface to examine the influence of the divalent ions: Mn^{2+}, Mg^{2+}, and Ca^{2+}. The Krafft temperatures of the pure divalent dodecyl sulfates are 16, 35, and 50 °C, respectively,[17−19] so Mn^{2+} is the only one of the three which can be studied at high concentration at room temperature. We have focused on Mn^{2+} and Mg^{2+} as both of these have sufficient solubility to allow divalent ions to outnumber Na^+ ions in the system. With one possible exception, addition of any of the three divalent ions did not induce a gross morphological change in the surface aggregates: long, thin parallel structures were observed at all concentrations studied. Instead, changes in the adsorbate period were observed together with an increase in the adsorbed layer thickness with increasing divalent ion concentration at low surfactant concentration. The uniformity in observed morphology was contrary to our expectation but permits the adsorbed state to be described by just two parameters: the aggregate period, and the thickness of the adsorbed layer.

Experimental Section

Sample Preparation. Water was prepared by distillation and then passage through a Milli-Q RG system consisting of charcoal filters, ion-exchange media, and a 0.2 μm filter. The resulting water has a conductivity of 18 MΩ cm^{-1} and a surface tension of 72.4 mJ m^{-2} at 22.0 °C. Sodium dodecyl sulfate, SDS (BDH, U.K., 99%), was recrystallized from ethanol. Investigations with this surfactant reproduced our previous work.[13] Analytical grade magnesium chloride 6-hydrate (BDH, >99%) was used as received. Manganese chloride 4-hydrate (BDH, >98%) was recrystallized from acidified ethanol. Calcium chloride 2-hydrate (Riedel-deHaën, 99%) was recrystallized from ethanol and then heated at 500 °C in air for 12 h to remove the water of crystallization and organic material. Ethanol (98%) was distilled before use. Adhesive tape was used to cleave a fresh sample of the basal plane of graphite for each experiment from a Pyrolytic Graphite Monochromator (grade ZYH, Union Carbide).

Surfactant Solubility. Investigations of the effect of divalent ions on dodecyl sulfate surface aggregates are limited by the precipitation of the hydrated divalent surfactant salt in a large region of the bulk solution phase diagram.[20,21] The low Krafft temperature of $Mn(DS)_2$ enabled us to measure the surface aggregate structure over a broad range of Mn^{2+} concentration (up to 0.44 M) in 1 mM SDS and to achieve a high ratio of divalent to monovalent ions. The Krafft temperatures of $Ca(DS)_2$ and $Mg(DS)_2$ are above room temperature, so the range of accessible concentrations is more restricted in these cases. The calcium chloride/SDS/water solution phase diagram has been studied at 25 °C, and in the absence of micelles, the solubility of DS^- in the divalent solution is simply governed by the solubility product.[20] The presence of micelles disrupts this equilibrium as the divalent ions associate with the micelles. This is evident in the change to a positive slope in the precipitation boundary curve.[22] That is, there is an increase in the tolerance toward divalent ions as the concentration is increased above the cmc.

The phase diagram of magnesium chloride/SDS/water was measured in the vicinity of the cmc of pure SDS and is shown in Figure 1. Each solution was equilibrated at 22 ± 2 °C for about 12 h and examined visually for a precipitate. There was no preliminary heating to 60 °C as performed in the previously published calcium phase determination.[20] The shaded region is the two-phase or precipitation region, while the remaining concentrations gave clear, single-phase solutions. The phase diagrams for Ca^{2+} and Mg^{2+} are very similar: both systems exhibit increased tolerance to the divalent cation with the onset of micellization. The primary difference is that a higher ratio of Mg^{2+}:Na^+ than Ca^{2+}:Na^+ can be obtained in single phase, clear solutions.

It is also important to ensure that the divalent ion is not partially or completely neutralized by ion pairing in solutions particularly for Mn^{2+} as the association with DS^- is low. The acid dissociation constant[23] for the $[Mn(H_2O)_6]^{2+}$ ion is $10^{-10.59}$ and we were unable to find any evidence for the association of

(12) Ducker, W. A.; Wanless, E. J. *Langmuir* **1996**, *12*, 5215.
(13) Wanless, E. J.; Ducker, W. A. *J. Phys. Chem.* **1996**, *100*, 3207−3214.
(14) Greenwood, F. G.; Parfitt, G. D.; Picton, N. H; Wharton, D. G. In *Adsorption from Aqueous Solution*; Weber, W. J., Matijevic, E., Eds.; American Chemical Society: Washington, DC, 1968; pp 135−144.
(15) Zettlemoyer, A. C. *J. Colloid Interface Sci.* **1968**, *28*, 343−369.
(16) Zettlemoyer, A. C.; Skewis, J. D.; Chessick, J. *J. Am. Oil Chem. Soc.* **1962**, *39*, 280−286.
(17) Moroi, Y.; Oyama, T.; Matuura, R. *J. Colloid Interface Sci.* **1977**, *60*, 103−111.
(18) Miyamoto, S. *Bull. Chem. Soc. Jpn.* **1960**, *33*, 371.
(19) Hato, M.; Shinoda, K. *J. Phys. Chem.* **1973**, *77*, 378.
(20) Bavière, M.; Bazin, B.; Aude, R. *J. Colloid Interface Sci.* **1983**, *92*, 580−583.
(21) Gerbacia, W. E. F. *J. Colloid Interface Sci.* **1983**, *93*, 556−559.
(22) Peacock, J. M.; Matijevic, E. *J. Colloid Interface Sci.* **1980**, *77*, 548−554.
(23) Burgess, J. *Metal Ions in Solution*; Ellis Horwood Ltd.: Chichester, England, 1978.

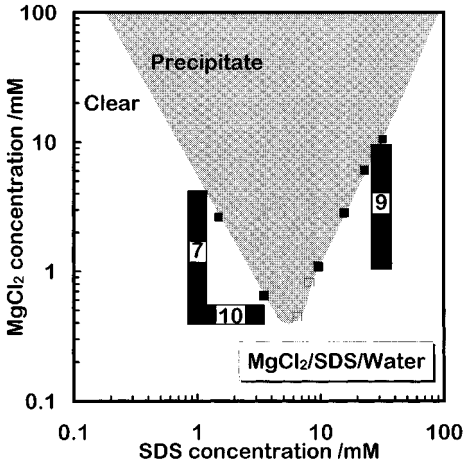

Figure 1. Phase diagram of $MgCl_2$/SDS/water at 22 ± 2 °C. The shaded area indicates solutions containing precipitates, and the white area represents the single phase solution region. Filled squares indicate where the boundary was accurately determined from both sides and open squares where measurements were made only on one side of the boundary. The remainder of the diagram is an extrapolation. The black bars show the composition of the solutions we have examined for surface aggregates, and the numbers refer to the figure in which the data are presented.

the chloride ion with Mn^{2+} except in the presence of strong acid. Thus, the doubly-charged cation is the dominant species in solution.

Microscopy. Images were captured using a Nanoscope III AFM[24] (Digital Instruments, CA) using silicon ultralevers (Park Scientific, CA) with nominal spring constants of 0.07 N m^{-1}. The ultralevers were irradiated for 40 min (~9 mW/cm^2 at 253.7 nm) in a laminar flow cabinet before use. All images presented are deflection images (showing the error in the feedback signal) with integral and proportional gains of between 1 and 2, and scan rates of 10 Hz. No filtering of images was performed other than that inherent in the feedback loop. Distances in lateral dimensions were calibrated by imaging a standard grid (2160 lines/mm), and distances normal to the surface were calibrated by measuring etch pits (180 nm deep).

All measurements were performed in the temperature range 25 ± 2 °C and in equilibrium with single phase surfactant solutions as described previously.[13] Quantitative data was taken from images in which the fast scan axis was perpendicular to the aggregate axis. Since our previous publication on SDS[13] we have learned that the dependence of aggregate period on scan angle is more complex than we originally thought. Scans which are not perpendicular to the aggregate symmetry axis often produce periods which are greater *or* smaller than perpendicular scans and these can be different in successive up and down scans. When the scan direction is normal to the aggregate axis, these effects are not observed. However, it must be stressed that the same morphology was observed at all scan angles.

In any AFM measurement it is important to appreciate that there will be some uncontrolled movement of the sample relative to the tip. A common manifestation is a slow drift of the sample in the plane normal to the tip. This drift is particularly obvious when making quantitative measurements of the distance between parallel features. For example, if one attempts to measure a period in the direction parallel to the slow scan axis, a relatively large period of time will elapse between measurements of parallel features. The effect of any uncontrolled tip−sample displacements will thus be magnified (see Figure 2a). For this reason we have made all quantitative measurements on images in which the symmetry axis was parallel to the slow scan axis. Under this condition, the period is determined for points measured closest together in time, and for points which are "flattened" together. When the symmetry axis is parallel to the slow scan axis, drift parallel to the fast scan axis will still cause up−down scan asymmetry and some error in the period as shown in Figure 2b. To avoid the comparatively smaller error induced by drift in this dimension, data were only recorded when the difference in orientation between up and down scans was less than 20°.

(24) Binnig, G.; Quate, C.; Gerber, G. *Phys. Rev. Lett.* **1986**, *56*, 930−933.

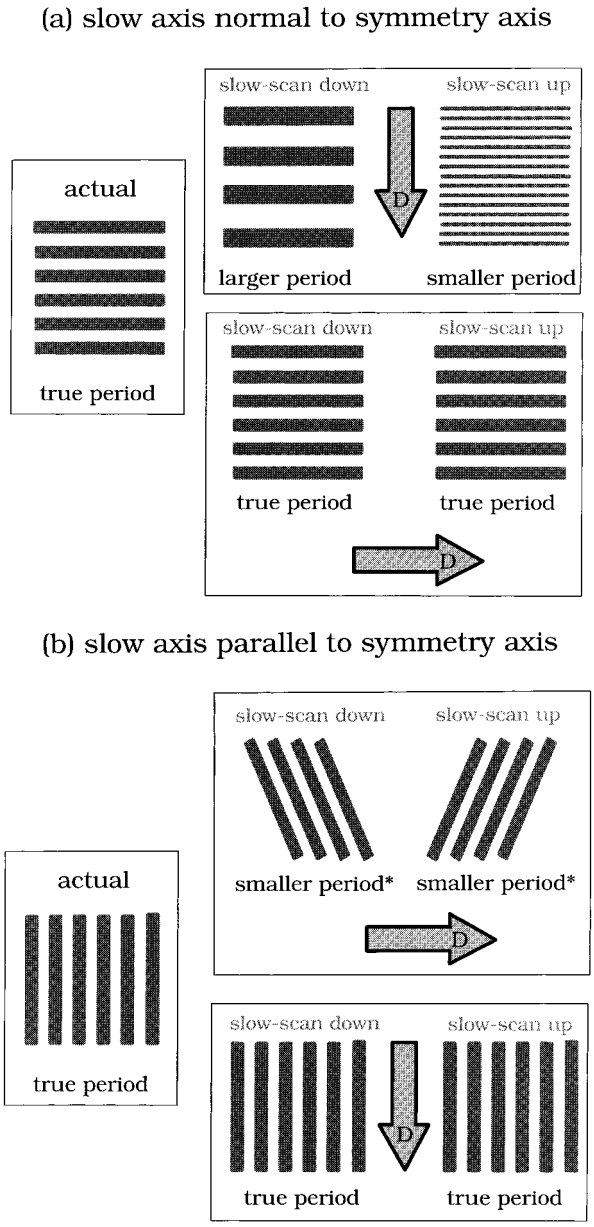

Figure 2. Schematic illustration of the effect of substrate-plane drift on the period of evenly spaced parallel features in an AFM image. The two simplest cases of slow scan axis normal (a) and parallel (b) to the symmetry axis are presented. Drift of the sample (arrow D) normal to the symmetry axis results in an error in the measured period, whereas parallel drift yields the true period. When the symmetry axis is at an intermediate angle, the relationship between the measured and true periods is a more complex function of drift. The asterisk indicates that the period is smaller when measured normal to the measured (in this case "apparent") symmetry axis.

Results and Analysis

General Features of Aggregation and Imaging. The morphology of the surface aggregates in the presence of Mg^{2+}, Ca^{2+}, and Mn^{2+} ions was similar to that observed in pure SDS solutions. That is, a regular array of linear, parallel features was observed, with no ends detectable except at the grain boundary with aggregates of a different orientation. Structures of a single period covered the entire graphite surface. An example of these features is shown in Figure 3 for a solution of 1 mM SDS and 3.2 mM

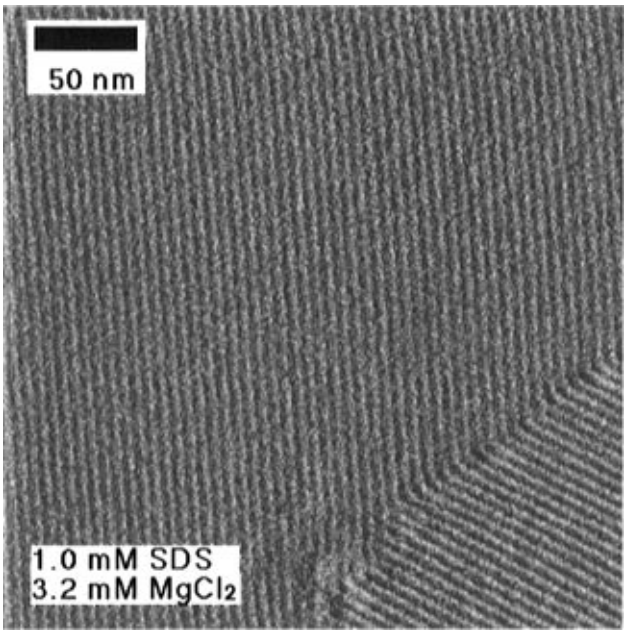

Figure 3. AFM image showing the one-dimensional periodicity of adsorbed dodecyl sulfate on graphite in aqueous solution of 1 mM SDS and 3.2 mM $MgCl_2$. In the lower right hand corner there is a region where the surfactant aggregates occur at a different orientation.

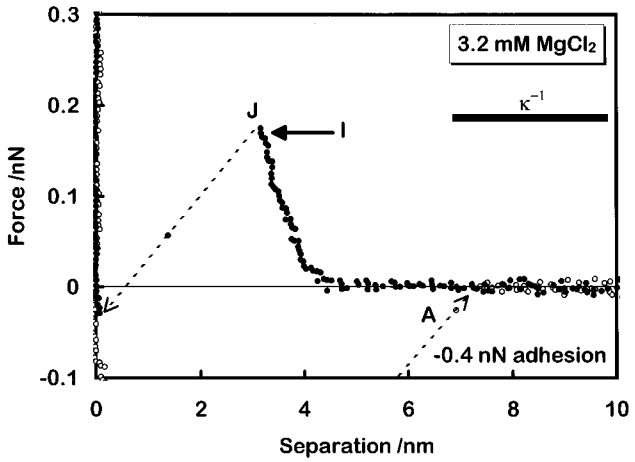

Figure 4. Normal force as a function of separation between a silicon ultralever and a freshly cleaved graphite surface in aqueous 1 mM SDS and 3.2 mM $MgCl_2$. The filled symbols show points measured as the tip approaches the sample and the open symbols show points on retraction of the tip from the sample. On retraction, the force extends to attractive forces beyond the range shown. A maximum attraction of −0.4 nN is measured, then an instability in the tip−sample separation occurs. The next equilibrium point is measured at 7.3 nm separation. In subsequent force-figures this behavior is summarized by the labeled adhesion. The symbols indicate the following: I shows the force at which aggregates were imaged, J is the separation at which the tip jumps toward the graphite surface because of mechanical instability, and A indicates the path of the tip as it leaves the surface. The separation, J, is a measure of the total thickness of the adsorbed layer on the tip and sample. Note that the imaging force and instability force are very similar, which causes difficulty in maintaining a constant separation (see Figure 6). The solution Debye length, κ^{-1}, is equal to the length of the solid bar.

$MgCl_2$. With one possible exception, AFM imaging only revealed changes in the period and of the adsorbed layer thickness, not a change in overall structure (e.g., a transition to a flat adsorbate layer). As found previously, the aggregate long axes occurred only in three orientations at about 60° to each another.

For every solution condition examined, the force between the AFM tip and the surfactant-coated sample was measured as a function of separation. A typical force curve at low surfactant concentration (1 mM) with added Mg^{2+} (3.2 mM) is shown in Figure 4. As in the pure surfactant solutions,[13] optimal resolution of the surface aggregates was obtained when the tip and solid substrate were slightly separated, with the tip very close to the adsorbed surfactant layer. The surface aggregates were sometimes visible at forces above which the surfactant is displaced when the tip moves normal to the surface, indicating that lateral motion of the tip stabilizes the surfactant on the surface.

The most salient parameter of the system is the period of the alternating high and low features, which can be precisely determined from a Fourier transform of an image. Figure 5 shows a schematic illustration of a cross section through a model of the tip−substrate interaction. For simplicity we have shown a semicircular cross section, but at this stage we do not have an accurate measure of the actual aggregate profile. In general, the surfactant may adsorb on the tip and on the sample and the aggregates on each may have different morphology because the tip and substrate have different shape and chemistry. This schematic illustrates that the period can be greater than the actual diameter of an adsorbed aggregate because the repulsive interactions between the aggregates can produce a finite separation. Previously it was shown[13] that in NaCl solutions that the period of adsorbed dodecyl sulfate structures decreases as the Debye length of the solution decreases. This scaling suggests that double-layer forces dominate the interaction between adsorbed aggregates. Screening of electrostatic repulsions between headgroups *within* an aggregate should lead to a *greater* diameter of an aggregate. Therefore, any

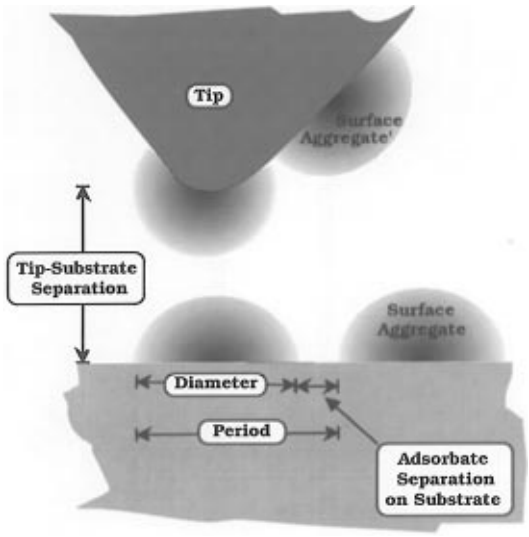

Figure 5. Schematic illustration of a cross section through our model of the tip−sample region in surfactant solution. Our measured parameters, the period, and the tip−substrate separation at the instability (thickness) are related to the model as follows: the period is the sum of the aggregate diameter and the aggregate separation on the substrate, and the thickness is the tip−substrate separation when the gap between the tip and substrate is occupied by surfactant aggregates only (no solution). It should be noted that in general we would expect that our separation and thickness parameters would be influenced by the presence of the tip and, in particular, by the force exerted by the tip.

measured reduction in *period* on addition of salt most likely corresponds to an even greater reduction in *inter-aggregate separation*.

Other than the period, the second parameter which is convenient to measure is the thickness of the adsorbed layer. The thickness was obtained from the normal force curve. It is commonly observed that when the tip approaches the sample there is a point at which the tip moves quickly, due to a mechanical instability, i.e., the positive gradient of the force is greater than the cantilever spring constant. There are several possible causes of this feature in a force-separation relationship, one of which is displacement of a surface layer. The work required to remove the surfactant from the gap between the tip and sample is manifest as a repulsive tip−sample force. As the surfactant is displaced, the tip−sample force quickly decreases, hence the rapid change in gradient. We have recorded the separation at which this instability occurs (e.g., at J in Figure 4) and assigned this value to the adsorbed layer thickness. This assignment is not unambiguous, because other forces can cause instabilities (e.g., attractive van der Waals forces) and because surfactant can be displaced from both the tip and solid substrate. The AFM tips are composed of silicon with a silicon oxide surface and hence are negatively charged in water. In pure SDS solution we were confident that DS^- did not adsorb to the tip, but the presence of divalent cations provides a mechanism for the anionic surfactant to adsorb to the anionic solid. In addition, the aggregate may be deformed by a significant load (compressive or tensile) when the instability occurs. A further difficulty associated with the assignment of a layer thickness is that the adsorbate may be distributed inhomogeneously across the substrate and it is not immediately obvious how this inhomogeneity is manifest in the measured force of interaction.

To summarize, we have chosen to parameterize our data in terms of the overwhelmingly dominant period in the Fourier transform, and the tip−substrate separation at which mechanical instability occurs.

Effect of Mg^{2+}. We have examined different concentration regimes within the single-phase region and observed a similar aggregate appearance in all regions measured with one exception (described later). The three regimes studied are labeled in Figure 1 by their figure numbers. This consists of a series at constant surfactant concentration above and below the cmc of pure SDS and a series at constant Mg^{2+} concentration near the minimum in the precipitation region. The behavior in $CaCl_2$ solutions is similar and will be described in this section.

Effect of Mg^{2+} below the cmc. Figure 6 shows the aggregates observed in 1 mM SDS and 4.1 mM $MgCl_2$. In this image, the aggregates are clearly visible in the lower half of the image. The upper half of the image was recorded with the tip in contact with the graphite, but the graphite lattice is too small to show on the image. The movement of the tip from on top of the surfactant to on top of the substrate occurred spontaneously and is a common occurrence. It is difficult to maintain the tip at constant separation or force because of dimensional changes in the microscope. The most disturbing of these are cantilever deflections due to small temperature changes. If such a bend occurs, it is registered as a force by the feedback loop, even though it is not arising from the sample. Thus, the tip−sample force can vary even when the feedback loop is operating perfectly. At this low surfactant concentration the aggregates are only visible over a small range of force (~0.05 nN) making it difficult to obtain an entire image without the tip contacting the substrate.

A summary of data for 1 mM SDS and various Mg^{2+} concentrations up to the solubility limit is shown in Figure 7. The addition of Mg^{2+} decreased the period of the surfactant aggregates, but the effect was not large. It is notable that near the precipitation boundary, the period did not decrease from 2.5 to 4.2 mM Mg^{2+} even though the Debye length decreased. This is in stark contrast to the behavior in Na^+ up to the limiting period of about 5 nm.[13] No adsorbed surfactant features were seen at the concentration labeled *no data*. Since the cmc of $Mg(DS)_2$ is 0.9 mM,[18] some of the concentrations investigated should be above and some below the cmc for particular Mg^{2+} concentrations.

The layer thickness increased from less than 0.5 nm at 0.45 mM Mg^{2+} to an average of 3.1 ± 0.6 nm above 1 mM Mg^{2+} as shown in Figure 7. This latter value is greater

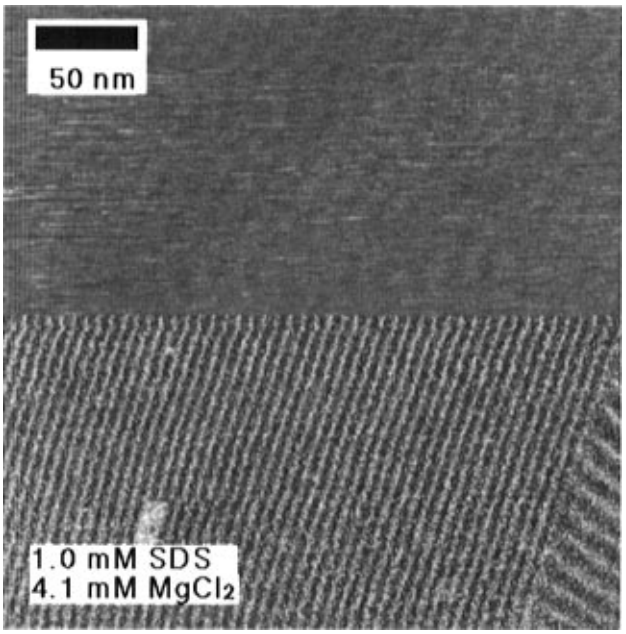

Figure 6. AFM image of dodecyl sulfate surface aggregates in aqueous solution of 1 mM SDS and 4.1 mM $MgCl_2$. The scan shows the surface aggregates in the lower half and then spontaneous drift into contact with the graphite. (The scan was started at the bottom of the figure). In the lower right hand corner, the aggregates have a different orientation. The occurrence of the larger period was explained in the Experimental Section.

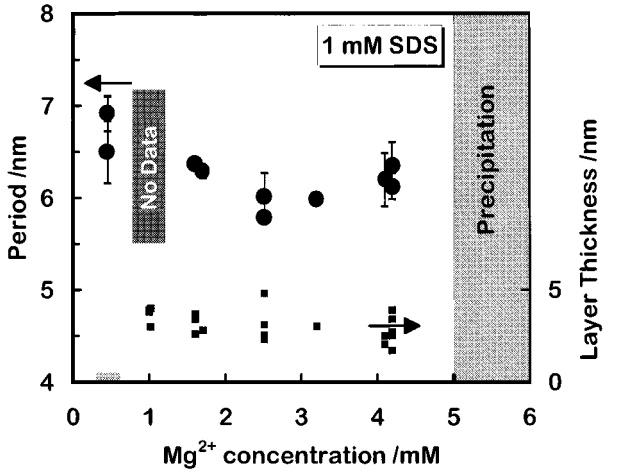

Figure 7. Effect of Mg^{2+} concentration on adsorbate period (circles) and layer thickness (squares) in 1 mM SDS (below the cmc of pure SDS). The period was measured from the Fourier transform of the image and the thickness from the separation J, the point of mechanical instability. The error bars show the full variation in the measured period at each concentration. For some concentrations, the error is smaller than the symbol size. At 1 mM Mg^{2+} no features were visible in the AFM image. At 0.45 mM Mg^{2+}, the layer thickness was <0.5 nm as indicated by the shaded bar.

than the thickness of 1.7 ± 0.7 nm previously measured for 2.8 mM SDS,[13] but it must be remembered that this thickness is the total thickness of adsorbed material on the tip and sample. On several occasions the adsorbed thickness was measured to be significantly greater after the solution had been left overnight. The overnight data are shown in Figure 7 and have also been included in the average thickness.

The normal force varied significantly as a function of Mg^{2+} concentration. The normal forces for the data in Figure 7 are shown in Figures 4 and 8. The interaction shown in Figure 4 is typical of the entire range 1.6−4.2 mM Mg^{2+}.

It is often convenient to think of the total force between the tip and sample as the sum of a number of components such as the van der Waals force, the electrostatic double-layer force, hydration forces, steric and confinement forces, and the surfactant displacement force. As we increase the Mg^{2+} concentration, we might expect any or all of these to alter, but we will begin our analysis by considering the electrostatic forces. Mg^{2+} can affect the double-layer force in two ways: adsorption will change the surface potential or the charge and thus the overall magnitude of the force, and Mg^{2+} in solution will alter the rate of decay of the force or Debye length, κ^{-1}. In water at 25 °C, κ^{-1} is given by the following equation:[2]

$$\kappa^{-1} = \sqrt{\frac{\epsilon\epsilon_0 kT}{e^2 \sum_i Z_i^2 \rho_i}}$$

where $\epsilon\epsilon_0$ is the permittivity of the solution, k is Boltzmann's constant, T is temperature, e is the electronic charge, Z_i is the number of electronic charges per ion and ρ_i is the concentration of each ion in solution in molecules m^{-3}. Scale bars on Figures 4 and 8 show the magnitude of κ^{-1} for each solution. In pure SDS solutions, a repulsive force with the predicted value of κ^{-1} was measured at each concentration. From Figure 8a it is clear that there is no large repulsive force with the predicted κ^{-1}. This strongly implies that the surface charge has fallen. At 0.45 mM Mg^{2+} there is no detectable repulsion before the instability, which indicates that the tip and sample have either no charge or opposite charge. At 1.0 mM Mg^{2+} (Figure 8b), there is a slight repulsion, suggesting that one or both of the surfaces has become charged or that the surface charges have become more similar. More work would be required to determine the surface charge on both the tip and sample at all concentrations, but the loss of the repulsive double-layer force and then an increase suggest that charge reversal has occurred. The behavior is consistent with both the tip and sample changing from negative to positive charge between 0 and 1 mM Mg^{2+}.

It would be very interesting to know the structure of the adsorbed layer at the point of zero charge, but unfortunately we were unable to measure any structure in the region of 1 mM Mg^{2+}. The repulsive barrier was too small to hold the tip distant from the sample for a reasonable interval and we are only left to conjecture whether there was no periodic structure or whether we just could not observe it. In 0.45 mM Mg^{2+}, clear images of long parallel surface aggregates were observed at the force shown by the arrow marked I (in Figure 8a). These aggregates are thus observed very close to or at the point of charge reversal. The force at 0.45 mM Mg^{2+} is quite different to the force at other concentrations: instead of one single displacement of the tip with increasing force, contact with the graphite substrate was achieved through a series of small displacements and was completed at a significantly greater force. In addition, the force at which these displacements occurred varied from measurement to measurement. The retracting curve was very similar to the approaching curve; that is, no significant adhesion was observed. The portrayal of the layer thickness at this concentration with a bar on Figure 7 represents the indistinct nature of the force close to zero separation.

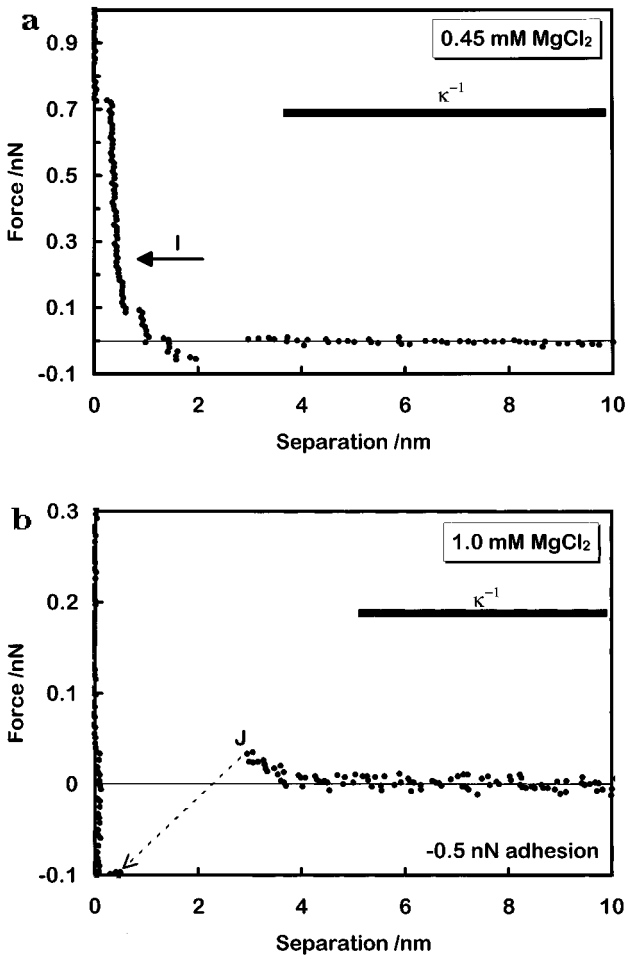

Figure 8. Normal force as a function of separation for two of the solutions of Figure 7. (a) Aggregates were resolved at the image force labeled I. The retracting curve is not shown since it was very similar to the interaction on approach (1 mM SDS and 0.45 mM $MgCl_2$). (b) Aggregates not resolved (1 mM SDS and 1 mM $MgCl_2$). Note that (a) and (b) are from experiments with different tips, so the magnitude of the forces cannot be directly compared.

Effect of Mg^{2+} above the cmc. At 30 mM SDS (above the pure surfactant cmc) the aggregate symmetry is independent of Mg^{2+} up to the precipitation limit, so we have again summarized our data in terms of the period and layer thickness. As shown in Figure 9, the period is unchanged from the pure surfactant value (5.2 nm) all the way to the precipitation boundary. The same period was also observed in 30 mM SDS for 0.1, 0.6, and 1.2 mM *calcium* chloride. Figure 9 also shows that the measured layer thickness was essentially constant at 2.6 ± 0.4 nm. However, on some occasions there was no instability in the force measured in the pure surfactant solutions.

Effect of SDS at Constant Mg^{2+} Concentration. The effect of SDS concentration on adsorbate period at constant, 0.45 mM Mg^{2+} is summarized in Figure 10. The point at 30 mM SDS is an interpolation of the periods measured at 0 and 1 mM $MgCl_2$. Interpolation is reasonable at 30 mM since the period did not vary with $MgCl_2$ concentration (Figure 9). There are three note-

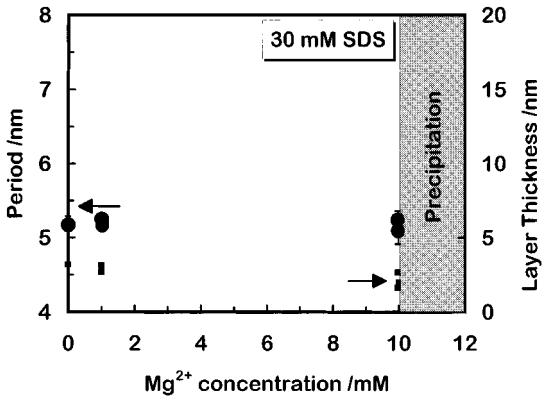

Figure 9. Effect of Mg^{2+} concentration on adsorbate period (circles) and layer thickness (squares) in 30 mM SDS (above the cmc of pure SDS).

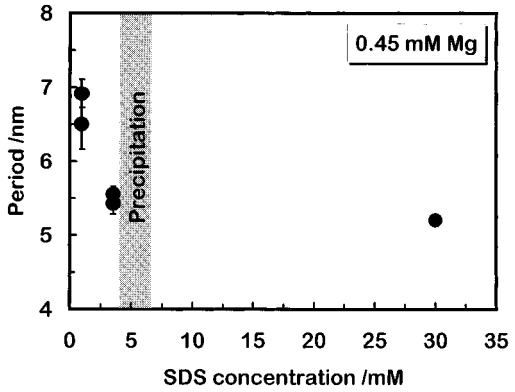

Figure 10. Effect of SDS concentration on adsorbate period in constant 0.45 mM Mg^{2+} (across the minimum in the precipitation region). The point at 30 mM SDS is interpolated from the measured values in pure surfactant and in 1 mM $MgCl_2$ which were essentially equal (Figure 9).

worthy effects here: the period decreases on the addition of surfactant indicating further adsorption, the precipitation region presents no significant disruption to the trend in adsorbate period, and the sac is lower in the presence of Mg^{2+} for we are clearly observing surface aggregates at 1 mM SDS whereas the sac was greater than 1.6 mM in pure SDS.[13]

Effect of Mn^{2+}. At 25 °C the solubility of $Mn(DS)_2$ is very high, so we are able to examine the effect of high Mn^{2+} concentrations (small Debye length) and a high ratio of Mn^{2+}:Na^+. The focus of our study is on 1 mM SDS to allow direct comparison with the Mg^{2+} data. The cmc of $Mn(DS)_2$ is 1.2 mM,[17] so the most dilute solution (1 mM SDS and 1.2 mM $MnCl_2$) is probably just below the cmc. Over the entire range of Mn^{2+} concentrations investigated (1.2 mM to 0.44 M), the adsorbed aggregates were long and thin as in pure SDS solutions. Examples of the dodecyl sulfate aggregates in the presence of low (1.2 mM) and high (242 mM) concentrations of Mn^{2+} are shown in Figure 11. The clarity of images in the Mn^{2+} solutions was generally lower than that observed in the pure surfactant and was a function of Mn^{2+} concentration. The clearest images were recorded in the range 20−240 mM Mn^{2+} and the least clear were obtained in the range 4−8 mM.

Changes in aggregation are summarized by the period and thickness measurements shown in Figure 12. The period of the aggregates decreases monotonically with bulk Mn^{2+} concentration. This is similar to the effect previously observed for Na^+,[13] but in contrast to the behavior in Mg^{2+} solutions (Figure 7). The layer thickness was 2.8 ± 0.5 nm above 10 mM and small and variable at lower concentrations. An additional feature of aggregation in

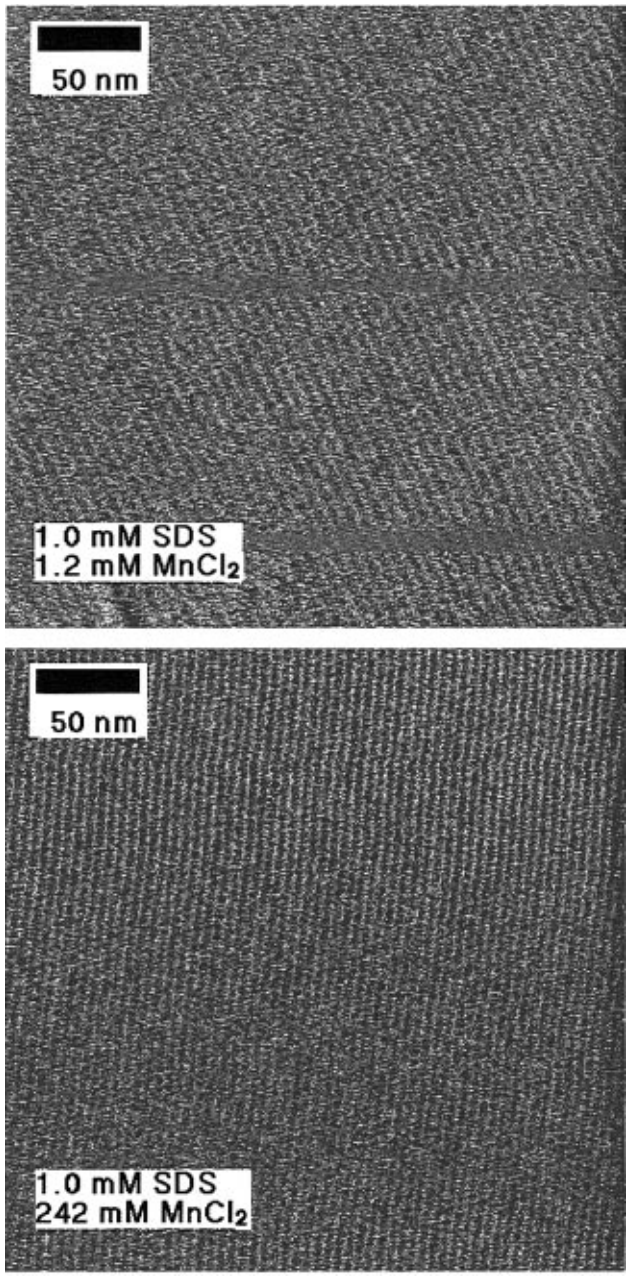

Figure 11. AFM images of dodecyl sulfate surface aggregates in aqueous solution of 1 mM SDS and (a) 1.2 mM and (b) 242 mM $MnCl_2$.

Mn^{2+} solutions is that the grain size is smaller than that in SDS alone: a boundary occurs in about half of all (300 nm)^2 images recorded.

The normal forces measured between the tip and the graphite substrate for several concentrations of added Mn^{2+} are shown in Figure 13. The graph at 242 mM is typical of data obtained at high concentration. There is a short-range repulsive force with appropriate Debye length leading up to a distinct instability at about 2.5 nm. This curve is reasonable for a charged surfactant layer similar to the schematic in Figure 5. As the bulk Mn^{2+} concentration is reduced, the barrier height decreases, until it becomes so small that it is difficult to maintain a stable image (e.g., 20 mM Mn^{2+}). At the same time the force behavior at much smaller tip−graphite separations (<0.5 nm) becomes much more complex. The tip passes through several variable instabilities which suggest layering at the surface. At the even lower bulk concentration of 4 mM Mn^{2+}, the barrier at 4 nm is gone, and there is only the series of barriers and instabilities at

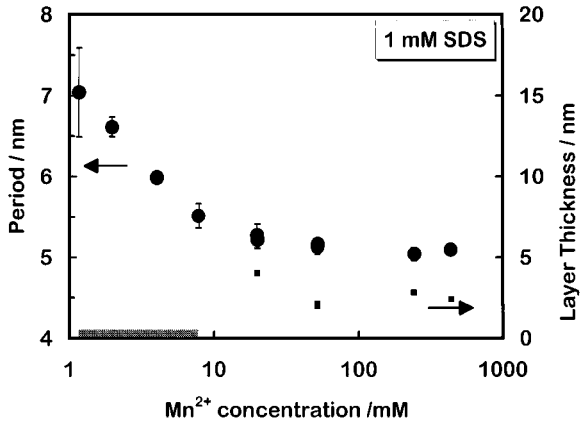

Figure 12. Effect of Mn^{2+} concentration on adsorbate period (circles) and layer thickness (squares) in 1 mM SDS (below the cmc of pure SDS). Note that the Mn^{2+} concentration scale is logarithmic. At low concentrations of Mn^{2+}, the layer thickness was less than 0.5 nm as indicated by the shaded region. The precipitation boundary was not determined.

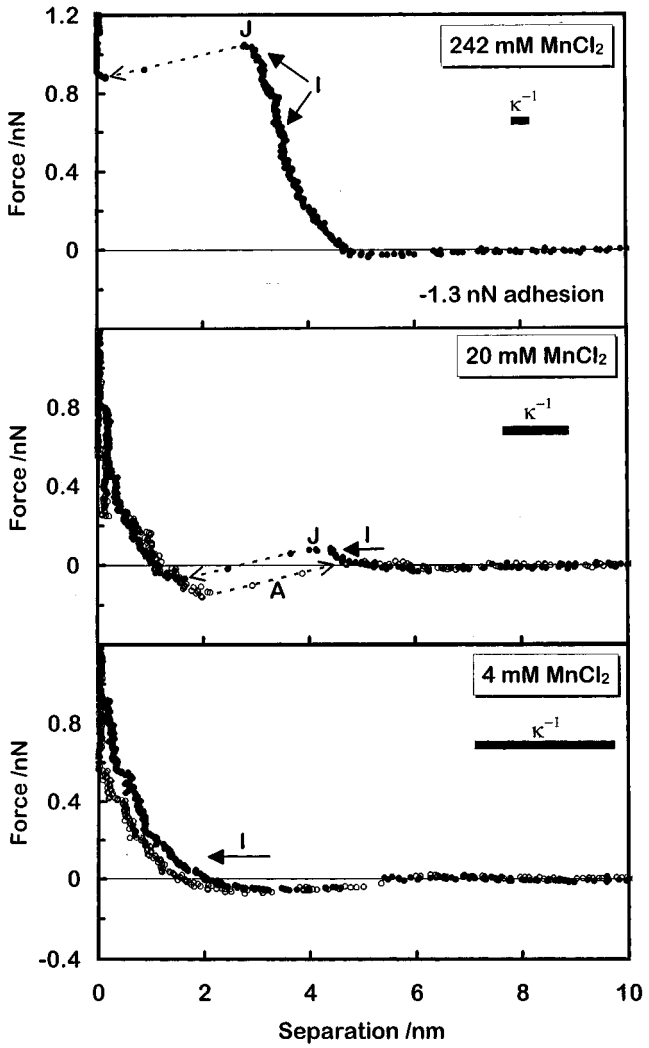

Figure 13. Normal force as a function of separation for three of the solutions of Figure 12 in 1 mM SDS with added Mn^{2+}. The force at which aggregates are resolved is indicated by the arrow, I. The three curves were recorded with the same tip, so the magnitude of the forces can be directly compared.

smaller separation. Sometimes there is a small attraction before the barrier (as shown). At these low Mn^{2+} concentrations, the aggregates were imaged at much smaller separation, but not at the steep portion where the

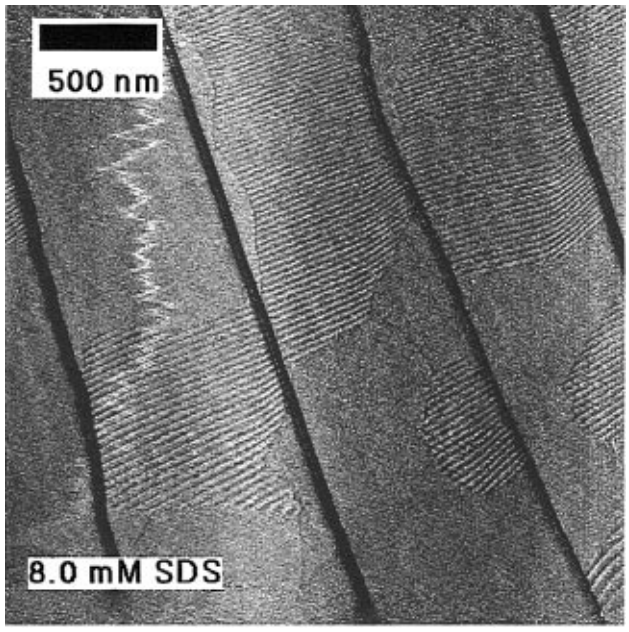

Figure 14. Large scale AFM image showing the superperiodicity sometimes observed. Periods of up to 30 nm are occasionally observed. Several steps in the graphite substrate are also visible. The solution concentration is 8 mM SDS.

series of instabilities suggests layering. The behavior at low concentration is similar to that observed in Mg^{2+}.

Anomalous Superperiodicity. A perplexing feature of surfactant-coated surfaces is that some images on the micrometre scale show large period features (up to 30 nm and variable) as shown in Figure 14. These were observed in pure SDS solutions as well as those containing added electrolyte although not on any consistent basis. There are several possible explanations for these larger scale features. The first is that they are an exaggeration of the effect of substrate-plane drift as discussed in the Experimental Section (Figure 2). However, that does not explain the patchy nature of the larger period regions nor that occasionally these larger period stripes are aligned parallel to the slow scan axis. The other notable feature of the larger period structures is that when part of the same region is viewed on a smaller image size, the ubiquitous standard-size surface aggregates are resolved, although these do not necessarily have the same orientation as the large period structures. The large period features are then seen on returning to the original scan size. This behavior is more consistent with an interference effect. Possible Moiré interference patterns have been observed with the scanning tunneling microscope,[25] and the superperiod observed here may be a manifestation of the same phenomenon involving substrate and tip adsorbate periodicity.

Discussion

The Aggregate Cross Section. One limitation of our work is that we have not been able to obtain a detailed picture of the cross section of the adsorbed aggregate. Our AFM images reveal periodic structure, but the amplitude of the height variation is typically about 0.2 nm, much smaller than the length of the surfactant molecule, or the jump-in distance that we have used to infer layer thickness (1.7−3.1 nm). Experimentally, the amplitude is a function of the speed of imaging and the strength of the feedback loop as expected. It is only a weak function of the imaging force and decays to zero when the gradient in the force−distance curve also drops to zero (at large separation). In

(25) Kuwabara, M.; Clarke, D. R.; Smith, D. A. *Appl. Phys. Lett.* **1990**, *56*, 2396−2398.

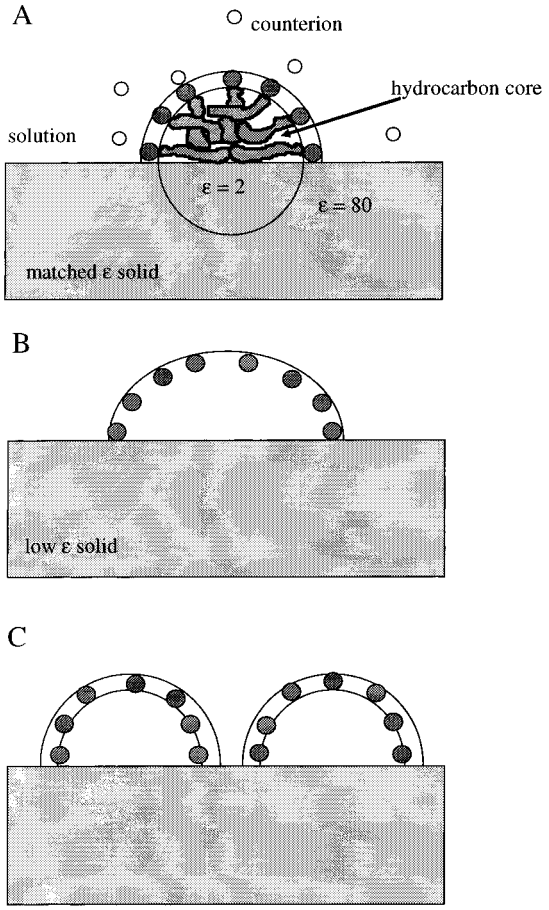

Figure 15. Schematic illustration of three possible surface aggregate cross sections consistent with AFM images of long parallel aggregates. Structure A shows a hemicircular cross section with matched dielectric constant of substrate and solution. More realistically, the inhomogeneity across the interface will result in deviations from constant curvature structures as shown by the top-flattened aggregate (structure B). Interaggregate repulsions on the substrate will tend to produce side-flattened aggregates such as structure C. The top of the aggregate may also be deformed by the tip. For clarity the counterions and hydrocarbon chains have not been shown in structures B and C.

principle, additional information should be obtained by taking a series of images at different forces or heights. We have tried this, but to little benefit in this system. The major limitation is that the tip radius is probably similar to or larger than the aggregate radius. This limits our resolution, leads to a lower apparent-curvature image (through tip convolution), and prevents us from accessing the high curvature regions between aggregates.

There are several surface aggregate cross sections which are consistent with both the AFM images as well as considerations of energy minimization. Two important energy considerations are to have equal energy for each molecule and to minimize the area of interaction between water and apolar groups. If we imagine a dielectrically matched hydrophobic substrate, these requirements suggest a hemicircular cross section with headgroups on the perimeter as shown in Figure 15A. The constant curvature of the hemicylinder ensures constant energy, and the headgroups along the perimeter lower the surface energy. Deviations from this shape may be caused by a more realistic substrate dielectric constant. For example, there will be a gradient of increasing dielectric constant away from a low ϵ solid, leading to a nonconstant curvature structure (Figure 15B). Similarly, interactions between aggregates will affect the curvature. Repulsive electrostatic interactions between aggregates on the surface should flatten the aggregate side (Figure 15C) and repulsive interactions with the tip will flatten the top of the aggregate.

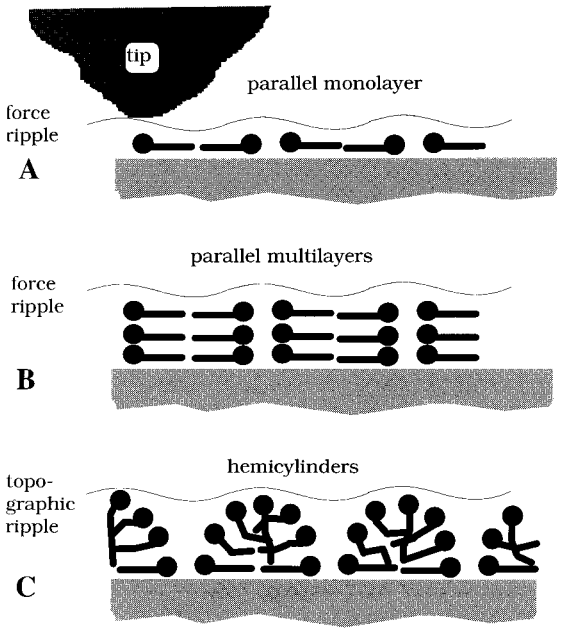

Figure 16. Schematic illustration of three possible aggregate structures consistent with the ripple recorded on scanning normal to the aggregate symmetry axis. The parallel monolayer (structure A) and the parallel multilayers (structure B) cause a force ripple through different interactions between the tip with the surfactant head and tail. The ripple arising from scanning the hemicylinders (structure C) arises from topographical variation.

A hemicircular cross section is not the only structure which is consistent with the observed images. Figures 16 shows three possible structures. In structures A and B, the force ripple is caused by differences in the way the adsorbed surfactant head and tail interact with the tip, and in structure C it is caused by differences in topography. In a previous publication,[13] we were able to eliminate the parallel monolayer structure, A, as a possibility for pure SDS solutions because the adsorption isotherm indicated that there were about five to seven molecules per cross section in the region investigated. However, the thin layer measured at low Mg^{2+} and Mn^{2+} concentration is consistent with a parallel monolayer.

The parallel multilayer structure, B (Figure 16), is more consistent with the forces measured in 0.45 mM $MgCl_2$ or 4 mM $MnCl_2$ and 1 mM SDS (Figures 8a and 13c): The multiple jump-ins imply that layers are being pushed out, and the lack of a long-range repulsion provides no barrier to multilayer adsorption. However, the variability in both the magnitude and width of the steps suggests that if multilayers are responsible, they are probably not as organized as shown in structure B. There were also cases where a small repulsive barrier was observed at about 0.3 nm (e.g., Figure 13b), but these may just indicate that the surfactant next to the graphite is strongly adsorbed and does not distinguish between structures B and C. At the higher concentrations of divalent ions where a significant repulsive barrier and a large jump-in were measured, the hemicylindrical structure, C, seems most likely.

In summary, AFM does not unambiguously distinguish between the structures shown in Figure 16. A transition from structure A or B to C with increasing Mn^{2+} or DS^- concentration is plausible on the basis of the measured interactions. Energetic considerations suggest that only headgroups should be facing the solution and thus that

the hemicylindrical structure, C, occurs at the higher concentrations investigated. Dielectric and interaggregate influences should cause deviation from constant curvature structures, offering the possibility of aggregate growth without large curvature changes.

Why Cylindrical Geometry? One of the central issues in the study of surfactant aggregates is the relationship between aggregate shape and the forces acting on the surfactant. In bulk solution, SDS forms approximately spherical micelles at 8 mM SDS, elliptical micelles at 80 mM SDS,[26] and there is some evidence for cylindrical micelles at 0.87 M.[27] At the interface between water and graphite, the aggregates observed by AFM always have one very long axis, and one axis which is of the order of the diameter of a bulk micelle at the cmc,[28] which is approximately twice the extended length of the surfactant.

When comparing a surface structure to a bulk structure in equilibrium, it is important to realize that the surface structure is usually at a much higher concentration.[11] For example, Greenwood *et al.*[14] found that the concentration of dodecyl sulfate at the interface between a 2.8 mM SDS solution and *graphon* was 2.1×10^{-10} mol cm^{-2}. If we approximate the thickness of this layer as the separation at which an AFM tip undergoes an instability (1.7 ± 0.5 nm),[13] we find a local concentration of about 1.2 ± 0.3 mol L^{-1}. At the same concentration in bulk, SDS forms cylindrical micelles, so the surface structure appears to be consistent with the bulk structure. However, this approach does not really answer the question posed in this section. Firstly, the surface concentration is usually high only in two dimensions so is not analogous to a bulk concentration, and secondly, this approach relegates the central contribution of the surface to a phenomenological concentration correction. That the surface does more than just concentrate the surfactant was clearly demonstrated when the observed structure of dodecyldimethylammoniopropanesulfonate (DDAPS) was found to be different on different substrates.[11] For dodecyl sulfate adsorption to graphite, we suggested previously[13] that a major contributor to the final structure was the driving force to minimize the contact area between the hydrophobic graphite and water. For a given surfactant concentration, hemicylinders cover a greater area of the graphite than hemispheres of the same diameter, and thus minimize the contribution from $\gamma_{\text{graphite-water}}$. This was confirmed for DDAPS by measurement of hemicylindrical aggregates on (hydrophobic) graphite and spherical aggregates on relatively hydrophilic mica.

Influence of Divalent Counterions. The aim of this work was to investigate the influence of divalent cations on the structure of adsorbed dodecyl sulfate aggregates. We expected that the presence of divalent ions would exert an influence on the electrostatic forces both within and between aggregates. Divalent ions would be expected to concentrate near highly charged bulk and surface micelles, and to reduce electrostatic repulsion or even to cause net electrostatic attraction between similarly charged groups by bridging or other ion-correlation forces. A transition from hemicylindrical surface aggregates to a flat monolayer of vertical surfactant molecules would be consistent with a significant reduction in the repulsion between headgroups. However, we did not observe this transition. No change in aggregate appearance was observed in the presence of Mg^{2+}, Mn^{2+}, or Ca^{2+}, even with solution Debye lengths as low as 0.26 nm when the ratio of Mn^{2+}:DS^- was 400:1. Rather, similar periodic aggregates were observed in all solutions investigated.

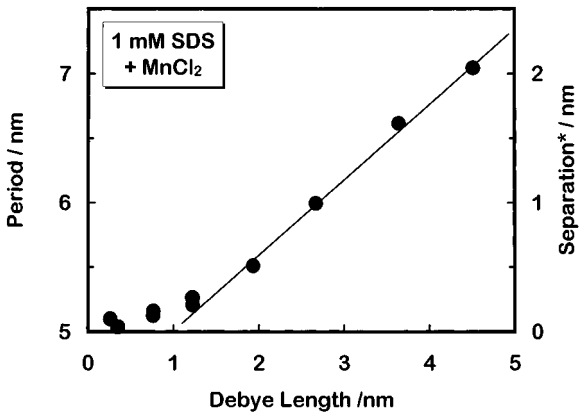

Figure 17. Data of Figure 12 plotted as a function of the solution Debye length, κ^{-1}. The period is found to be a linear function of the Debye length until the limiting period of about 5 nm is approached. The straight line is a guide to the eye. The right axis (separation*) shows the measured period minus the limiting period and is an approximation of the interaggregate separation.

Variation between the bulk aggregate shape of surfactants with monovalent and divalent ions appears to be system specific. In some cases, divalent counterions cause gross aggregate shape-changes (e.g., refs 5 and 29) or even precipitation (e.g., ref 20) while in others they have little or no effect (e.g., octyl sulfate[7] and hexadecyltrimethylammonium[8] ions) as was observed here. When present, divalent ions will reduce the electrostatic repulsion between headgroups which opposes aggregation and imparts curvature on the aggregate. Thus, simple electrostatics suggest that divalent ions will cause a decrease in aggregate curvature. Ion−ion correlation effects will further reduce the repulsion and in some circumstances lead to an attraction between headgroups. The partitioning of divalent ions near the charged micelle surface will, however, be somewhat reduced compared to the equivalent interaction in bulk because of the low-dielectric micelle interior.

The same arguments can be used for surface aggregates: divalent ions should reduce the curvature of surface aggregates. There will also be a dielectric discontinuity due to the additional phase. Low dielectric substrates will repel divalent ions, but for the work presented here we have the complication that graphite is a good conductor in the plane parallel to the surface.[30] A conductor produces image charges of opposite sign and should lead to a concentration of divalent ions. Thus it is surprising that divalent ions have such a weak effect.

Aggregate Period: Mn^{2+} Ions. Mn^{2+} ions reduce the period of aggregated DS^- molecules on graphite. For both Mn^{2+} and Na^+ there appears to be a limiting period of about 5 nm which may represent the diameter of the aggregates. Above this limit, the period increases linearly with Debye length even through the range of surface charge reversal. This is clearly shown in Figure 17. As stated previously,[13] the observation that the period changes linearly with the Debye length implies that changes in period are dominated by the interaggregate separation rather than by a change in aggregate curvature.

(26) Zhao, J.; Fung, B. M. *Langmuir* **1993**, *9*, 1228−1231.
(27) Reiss-Husson, F.; Luzzati, V. *J. Phys. Chem.* **1964**, *68*, 3504−3511.
(28) Hayter, J. B. In *Proceedings of the International School of Physics: Physics of Amphiphiles: Micelles, Vesicles and Microemulsions*; Degiorgio, V., Ed.; Elsevier: Amsterdam, 1985; pp 59−93.
(29) Tilcock, C. P. S.; Bally, M. B.; Farren, S. B.; Cullis, P. R.; Gruner, S. M. *Biochemistry* **1984**, *23*, 2696−2703.
(30) Bowen, H. J. M. *Properties of Solids and their Atomic Structures*; McGraw-Hill: London, 1967.

A decrease in Debye length should decrease all electrostatic repulsions and thus cause an increase in aggregate diameter and a decrease in interaggregate separation. This behavior is observed in bulk for the hexagonal phase of SDS.[31] The observed decrease in period at the surface implies that the change in interaggregate separation is the dominant effect for Mn^{2+} and Na^{+}. Since both the separation and diameter can change individually, we cannot determine either, but the limiting period of 5 nm provides a rough upper bound for the diameter. The right axis of Figure 17 shows the period minus 5 nm and is an indication of the separation between aggregates. At long Debye lengths, these values will be underestimates because of the smaller aggregate diameter.

In the limit of an infinitely large solution reservoir, the equilibrium spacing of the aggregates on the surface of graphite is due to a minimum in the energy as a function of separation. To calculate the energy, we need the product of energy (as a function of separation) for each aggregate and the total number of aggregates. The total number of aggregates is simply given by $L/(D + S)$ where L is the length of surface normal to the symmetry axis, D is the aggregate diameter, and S is the separation. By analogy to DLVO theory, we shall consider the force between each pair of aggregates to be the sum of a (usually) repulsive double-layer force and an attractive surface energy force which seeks to minimize the exposure of graphite to water. (At high divalent ion concentrations, attractive ion-correlation forces and repulsive steric/confinement forces may become more important). The total attractive energy per unit length along the symmetry axis, E_l, is given by

$$E_l(S) = \frac{L}{D + S} D(\gamma_A - \gamma_S)$$

where γ_S is the substrate−solution surface energy, γ_A is the sum of the substrate−aggregate and aggregate−solution surface energies, the latter weighted for its greater area, and the zero of energy is where the graphite is covered in water. Note that E_l is inversely proportional to the period $(D + S)$, not proportional as stated previously.[13]

To date, we have not been able to derive an analytical result for the electrostatic energy or to fit an energy which together with the surface energy term produces an equilibrium separation proportional to Debye length. However, the linear relationship between equilibrium period and Debye length for both Mn^{2+} and Na^{+} suggests that there may be a simple analytical form.

The correlation between aggregate period and the solution Debye length suggests that the aggregate spacing is controlled by electrostatic forces. If the spacing is controlled by electrostatic forces, then we might also expect that the observed rigid alignment of aggregates is also caused by electrostatic forces. Possible reasons for alignment are a steep minimum in the plot of energy as a function of aggregate separation and/or a high bending modulus for individual aggregates, both of which should be influenced by electrostatic forces. Thus it is somewhat surprising that strong alignment of aggregates is observed over the entire range of Mn^{2+} concentrations (e.g., Figure 11).

Aggregate Period: Mg^{2+} Ions. In contrast to Mn^{2+} or Na^{+}, Mg^{2+} ions do not cause a linear decrease in observed period with Debye length, or even a limiting period of ∼ 5 nm (Figure 7). At low Mg^{2+} concentrations, the period decreases, and then remains constant or even increases. On the basis of the model that the period is the sum of the aggregate diameter and separation and that the separation decreases with ion concentration, this implies that the diameter of the aggregate increases in the range 2.5−4.2 mM. This is our only evidence of a decrease in aggregate curvature with the addition of divalent ions and is not conclusive.

At surfactant concentrations greater than the cmc, the adsorbate period was invariant on the addition of both Mg^{2+} and Ca^{2+}. This indicates either no further adsorption of surfactant or, alternatively, a change that is not detectable using AFM. These observations are consistent with those made in SDS with added NaCl in which a limiting period was reached above the cmc.[13] We have also observed similar aggregates with a period of 5.2 nm in aqueous solutions of 18 mM LiDS. Thus a variety of different counterions have been observed to have no effect on the surface aggregation of dodecyl sulfate on graphite above the cmc.

Thickness Changes. There are many factors which could influence our measurement of layer thickness, but it is nevertheless beneficial to consider trends in this parameter because an increase in layer thickness indicates further adsorption without the necessity for any change in the AFM image.

In 1 mM SDS both Mn^{2+} and Mg^{2+} exhibited two relatively distinct regimes above and below a critical concentration. Above 20 mM Mn^{2+}, there is a distinct barrier on approach of the tip to the sample which occurs at several nanometers of separation and is consistent with the existence of surface aggregates of similar thickness. Below 20 mM Mn^{2+} the tip approaches the sample without a barrier of the appropriate thickness for a hemicylinder and then encounters a series of force barriers (<1 nm) which are suggestive of layering at the surface. At 20 mM, it was possible to image aggregates at a separation of several nanometers, but there is still the series of barriers at low concentration. This evidence is consistent with the adsorption of hemicylinders (Figure 16C) at high Mn^{2+} concentrations, and a layered structure more like parts A and B of Figure 16 at lower Mn^{2+} concentrations. At 20 mM the force required to remove the large aggregates (at 4 nm) is insufficient to remove the layer closest to the graphite, so the steps at small separation are still observed. At higher Mn^{2+}, it is possible that there is still a tightly fixed bottom layer but that the force required to push through the top of the aggregate is now so large that the bottom layer is removed in the same action. The behavior in Mg^{2+} is similar, except that the transition from a thin layer to a thick layer (hemicylinders) occurs at lower concentration (∼1 mM Mg^{2+}). The structure at 1 mM Mg^{2+} remains difficult to determine, as there is a very small barrier at 3 nm, but we were not able to observe periodic structures at this separation or to hold the tip at a smaller separation. We are thus unable to describe the structure or even to say whether the barrier is due to a surfactant layer or to a small electrostatic force. It is in this low surface-charge regime where we might expect to observe a reduction in aggregate curvature due to the loss of electrostatic repulsion between headgroups, but the imaging conditions are so poor that it is not possible to prove the existence of a flat adsorbate layer.

Comparison to Adsorption Isotherm: Ca^{2+}. Adsorption isotherms have been measured for SDS on graphon in the presence of Ca^{2+}. (There is no data available for Mg^{2+} or Mn^{2+}.) The isotherms show that at 17 mM DS^{-}, Ca^{2+} can double the surfactant adsorption density.[16] Over the same range of added Ca^{2+} in 30 mM DS^{-}, we were unable to detect any morphological, period,

(31) Husson, F.; Mustacchi, H.; Luzzati, V. *Acta Crystallogr.* **1960**, *13*, 668−677.

or thickness changes. That is, we have no evidence for an increase in adsorption in this range of surfactant concentration.

Surface Aggregation Concentration. The lowest bulk surfactant concentration at which surface aggregation is observed by AFM has been termed the surface aggregation concentration (sac). In pure SDS solutions the sac was between 1.6 and 2.8 mM.[13] For Na^+, Mg^{2+}, and Mn^{2+}, we have only obtained upper bounds for the sac; they are 1.6 mM (160 mM Na^+), 1 mM (0.45 mM Mg^{2+}), and 1 mM (1.2 mM Mn^{2+}), respectively. As in bulk, surface aggregation is promoted by a decrease in headgroup repulsions in the presence of added electrolyte.

Relationship between Aggregate Symmetry and Substrate Symmetry. The symmetry axes of the dodecyl sulfate aggregates on graphite both with and without added electrolyte occur in only three directions. That is, the adsorbed dodecyl sulfate aggregates are oriented with respect to the hexagonal substrate beneath. The specific orientation has been reported by Manne *et al.*[9] for hexadecyltrimethylammonium bromide (CTAB) on graphite, who suggested that the adsorption was epitaxial. If this was indeed the case, we would expect that the aggregate period should be quantized by the unit cell of the graphite surface which we measure to be 0.25 nm. We do not observe quantization within a single region, from region to region, or between different solution conditions. An alternate reason for the orientation is alignment of the aggregates with step edges.[13] Step edges are aligned with the graphite lattice and provide a natural alignment for the long aggregates, as well as a suitable nucleation site. Evidence for this explanation is provided by images of CTAB on gold which show strong alignment of aggregates along step edges.[32]

Conclusions

The addition of the divalent ions, Ca^{2+}, Mg^{2+} and Mn^{2+}, to sodium dodecyl sulfate solutions does not cause a gross change in the shape of aggregates adsorbed to the surface of graphite. Divalent ions do enhance adsorption: they lower the surface aggregation concentration and increase the adsorption density, as measured by the aggregate period. Force curves also show that an increase in the concentration of divalent ions promotes a transition from a thin (<0.5 nm) to a thick (>3 nm) layer on the surface. The fact that the period of the aggregates in Mn^{2+} scales with the Debye length demonstrates that electrostatic forces are important and suggests that the enhanced adsorption occurs via a reduction in the charge−charge interactions which hinder aggregation. This work provides further evidence that the process of surface aggregation is affected by similar interactions to those which influence bulk aggregation but that surface structures depend on the details of the individual substrate.

Acknowledgment. Our thanks go to Charles Clarke and Dirk Bokern for useful discussions and to George Petersen for the gift of the ultralevers. This work was funded in part by the NZ Lottery Science Commission (Ap38518) and by an Otago Research Grant.

LA960861E

(32) Manne, S.; Jaschke, M.; Butt, H. J.; Gaub, H. E. Submitted for publication in *Langmuir*.